4. Bioactivity-guided isolation of Vasaka

4.1. Experimental work

4.1.1. Chemicals

Amyloid beta (Aβ), scopolamine, donepezil, acetylthiocholine iodide, butyrylthiocholine iodide, DTNB, AChE, and BuChE were purchased from Sigma-Aldrich, USA. DPPH (2,2-diphenylpicrylhydrazyl) was procured from TCI chemicals, India. Rat ACh ELISA kit was obtained from Krishgen biosystems, India. All other chemicals and solvents were purchased from local suppliers.

4.1.2. Extraction and Fractionation

The shade-dried and hand-crushed powdered leaves of *Adhatoda vasica* Nees. (dehydrated vasa/vasaka/Malabar nut) were purchased (Batch no. MC/ADA/2/21) from Vedic vatica private limited, Chhattisgarh, India. A simple maceration technique was executed to get *Adhatoda vasica* Nees. methanolic extract (AVME) by adding 1 kg leaves power into 3 L of methanol. After 72 h, extract was filtered and concentrated under reduced pressure (rotary evaporator). This extraction process was repeated three times. Further, AVME (100 g) was dissolved into 200 mL water and transferred into a separating funnel for solvent-solvent extraction process. These fractions were prepared using organic solvents (hexane, toluene, ethyl acetate, dichloromethane (DCM), and butanol) which are selected based on polarity index i.e., non-polar to polar organic solvents to get all nature of compounds. The obtained fractions from each solvent were concentrated and dried under reduced pressure using rotary evaporator (Figure 4.1). The resulting crude samples (semi-solid) were transferred into a petri dish and calculated the yields of each extract/fraction using following formula [Percentage yield =

(weight of the plant material grams – weight of obtained crude extract or fraction in grams) / 100].

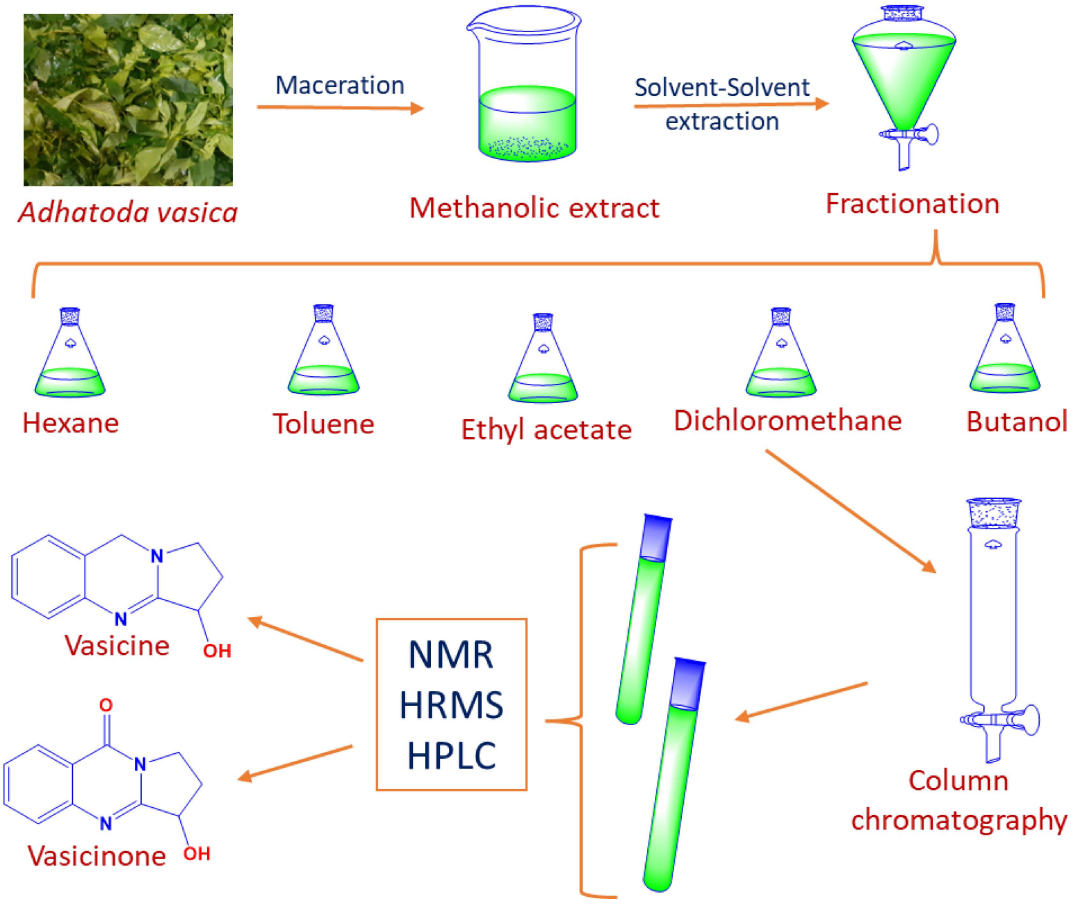

Figure 4.1. Process of bioactivity-guided fractionation of Vasaka

4.1.3. Cholinesterase inhibition assay of vasaka extract and fractions

Cholinesterase (AChE and BuChE) inhibitory activity of AVME and fractions, were evaluated by *in vitro* enzyme assay method [168]. In this assay, stock solutions (1 mg/mL) of AVME/fractions were prepared by dissolving samples into biological grade DMSO. Further, six different concentrations (200, 100, 50, 30, 20, and 10 µg) were prepared using phosphate buffer 7.4. to assess IC_{50}. The test samples with different concentrations were incubated with 100 µL of DTNB (0.0005 M) for 10 min, followed by addition of enzyme 50 µL of AChE/BuChE (0.5 U mL^{-1}) and incubated for another 30 min. Further, 20 µL of substrate ATCI (0.00375 M) was added for AChE test and 20 µL of substrate BTCI was added for BuChE

assay. The absorbance was measured at 415 nm, by SpectraMax M5 multi-mode microplate reader, US. In this assay, blank readings were measured using 2 µL biological grade DMSO instead of test samples. The standard drug donepezil served as a reference compound.

4.1.4. Isolation of active constituents

DCM fraction was selected for isolation of phytoconstituents on basis of cholinesterase inhibition and DPPH antioxidant activity results. The bioactive compounds were isolated using column chromatography technique. The sample was prepared by dissolving DCM fraction (10 g) into 20 mL of DCM. Followed by addition of sufficient amount of silica gel (60-120 mesh) and evaporated under reduced pressure (rotary evaporator) to get dried powder (extract bound with silica gel). Further, column was packed with silica gel (60-120 mesh) by preparing slurry in hexane; then, slurry was poured into column by tapping column to avoid column silica breaks and air gaps. The mobile phase solvents were used as hexane, ethyl acetate, dichloromethane, and methanol. The concentrated DCM fraction was loaded into column and mobile phase flow started with low polar solvent hexane (100 % hexane). Followed by increasing polarity using ethyl acetate, then dichloromethane, and finally 10 % methanol was run by gradually increasing polarity (gradient method). The obtained elutes from column were collected into 100 mL conical flasks and dried under reduced pressure (rotary evaporator). Each elute was evaluated by thin-layer chromatography (TLC) using precoated TLC silica gel 60 F_{254} and mobile phase polarity set to DCM: methanol (90:10). Resulting TLC plates were observed under the iodine chamber, UV light (254 nm), and Dragendorff's reagent solution for detection of alkaloids.

4.1.5. Structural characterization of constituents

The isolated compounds (VAS and VA) from DCM fraction were characterized by ATR, ^{1}H NMR, ^{13}C NMR, HRMS, and HPLC techniques. The ATR (Bruker Alpha, Germany)

fingerprints were taken and interpreted in functional groups present in the compounds. Further, Nuclear magnetic resonance (^{1}H, ^{13}C NMR) studies were performed using Bruker advance (Bruker Bio spin International AG, Germany), 500 MHZ (^{1}H NMR), and 125 MHZ (^{13}C NMR), in this experiment TMS served as an internal standard. Preparation of NMR samples, $CDCl_3$ solvent was used. Furthermore, the isolated compounds purity was estimated with the help of HPLC (waters 1500 series system). The working concentration of samples (100 µg) was prepared in methanol; then, passed through a 0.45 µm membrane filter. The following HPLC conditions were maintained: Lichro CART 250-4 C_{18} column, injection volume (10 µL), mobile phase uses as methanol and water (9:1) (pH 2-3 adjusted with acetic acid), flow rate (0.8 mL/min), PDA detector 2998 (280 nm). The chromatogram data was analyzed, using waters breeze software. The total area under all peaks in the chromatogram were calculated includes peaks corresponding to impurities, solvents, and any other compounds present in the sample. Further, total peak area of specific compound was calculated by breeze software using formula, Percentage Purity = (Area of the Peak of Interest / Total Area of All Peaks) x 100. Further, high-resolution mass spectrometry (HRMS) studies were carried out by SCIEX. X500R QTOF, US at the Department of chemistry, Banaras Hindu University, Varanasi to estimate molecular mass of compounds.

4.1.6. Drug-likeness, ADME, and toxicity predictions

The drug-likeness, ADME, and toxicity properties of VAS and VA were predicted using online software tools swissADME (http://www.swissadme.ch/) [169] and preADMET [170] (https://preadmet.qsarhub.com/). Drug-likeness properties of compounds were analyzed through Lipinski rule of 5. Further, ADME properties of the isolated compounds were predicted by using Swiss ADME software.

4.1.7. Molecular docking studies

The crystal structure of AChE co-crystallized with donepezil (PDB ID: 4EY7) [171] and BuChE complexed with tacrine (PDB ID: 4BDS) [172] was downloaded from the protein data bank (PDB) (https://www.rcsb.org/) [173]. These proteins were prepared by removing unwanted chains, water molecules, and other heteroatoms. In addition, quality of protein was evaluated by analyzing the results from Ramachandran plots using precheck software (https://saves.mbi.ucla.edu/). Further, structure of ligands (VAS and VA) was drawn on Perkin Elmer Chem 3D 20.1.1 software, and ligand energies were minimized.

After completion of above sequential steps, Auto dock 4.2 [174] software was used for further docking studies. The prepared protein structures and ligand structures were separately saved into auto dock supported format i.e., pdbqt file format. Further, grid box was fixed and saved with the help of reference compound donepezil/tacrine interaction with active site amino acids. Followed by docking files were created by following parameters i.e., search parameters set to genetic algorithms (GA runs set to 100 ns), docking parameters set to default parameters, and output file saved into Lamarckian GA (4.2). The docking results were analyzed under analyze window by clicking play rank by energy. Moreover, ligands have interacted with amino acids profile (2D and 3D) images were generated using BIOVIA Discovery studio visualizer [175].

4.1.8. Molecular Dynamic simulations

The molecular dynamics studies were performed on VAS/VA using Desmond (Maestro-Desmond) software tool [176]. The binding interaction profile and stability of the docked ligands under physiological conditions, 50 ns MD simulations were carried out at AChE active site. In these studies, TIP3P was selected as a solvent model, 10 A° cubic box, and minimized the volume. Further protein energy minimization was done by 300 ns. The system was prepared by system builder and it was neutralized by adding salt 0.15 M of Na^{+} and Cl^{-} ions. Further,

molecular dynamics simulations were carried out up to 500 frames with NTP enabled system, and temperate was set to 310 K with 1 bar pressure. The processed results were analyzed under simulation interaction diagram panel of Desmond.

4.1.9. Free-radical scavenging assay

2,2-diphenylpicrylhydrazyl (DPPH) assay was performed to study the antioxidant potential of AVME/fraction and isolated bioactive compounds. Various concentrations of AVME/fraction (500, 200, 100, 50, 30, 20, and 10 µg) and VAS/VA/ascorbic acid (200, 100, 50, 30, 20, and 10 µM) were made in methanol [177]. Further, test samples (75 µL) of various concentrations were added to 96-well plates, and to this 75 µl of DPPH (100 µM) was added. Then, samples were incubated at 37° C for 25 min. and absorbance was measured at 520 nm wavelength using a microplate reader (SpectraMax M5, US). In this study, Ascorbic acid (AA) served as a reference compound, and blank readings were taken by using methanol in the place of test samples. The reducing capacity of DPPH was calculated using following equation, reducing percentage = [(absorbance of control) - (absorbance of the test)/ (absorbance of control)] × 100.

4.1.10. Cholinesterase inhibition assay

Cholinesterase (AChE and BuChE) inhibitory activity of isolated compounds was evaluated using above-described procedure [168]. Six different concentrations (0.01, 0.1, 1.0, 10, 20, and 40 µM) were prepared for each compound (VAS/VA) to assess IC_{50}. The donepezil was used as a reference compound. The absorbance was measured at 415 nm, by multi-mode microplate reader (SpectraMax M5, US).

4.1.11. Propidium iodide displacement assay

Propidium iodide displacement assay was carried out to evaluate binding mode of test compounds at PAS site of AChE [177,178]. A solution of eeAChE 5.0 U/mL of 150 µL was incubated with or without test compounds with various concentrations of VAS (10, 20, and 30 µM), VA (30 µM), and DPZ (20 µM) for 6 h at room temperature (24°C). Followed by, addition of propidium iodide (final volume consists of 20 µM) and incubated for 20 min. The fluorescence intensity was measured at 535 nm (excitation) and 595 nm (emission) using a microplate reader (SpectraMax M5, US). The blank was measured using DMSO instead of test samples. The percentage inhibition results were calculated using the formula: 100-($IF_i/IF_0 \times 100$); where IF_i and IF_0 are fluorescence intensities with and without inhibitors respectively.

4.1.12. PAMPA-BBB Assay

The blood-brain barrier (BBB) permeation is a prerequisite condition for the drugs acting on CNS. The BBB permeability of test compounds (VAS and VA) was tested through a parallel artificial membrane permeability assay (PAMPA) [168,179]. Porcine brain lipid (PBL) 4 µL dissolved in dodecane (20 mg/mL of PBL in dodecane) was coated on the bottom of the porous filter disks of receptor plates. The test compounds were prepared in DMSO and further diluted with PBS buffer (pH 7.4) to get a final concentration of 25 µg/mL. Further, the donor plates (pore size 0.45 mm) were filled with 200 µL of test solution. The acceptor plate was placed on a donor plate-like sandwich and incubated for 18 h at room temperature. After, test compounds absorbance was measured at 280 nm by microplate reader (SpectraMax M5, US). A concentration of 30 µM of VAS and VA was used in this study.

4.1.13. Aβ inhibition activity

The assessment of Aβ aggregation inhibition activity was evaluated through thioflavin T assay [168]. The following concentrations were used viz., 10, 20, and 30 µM for VAS, 30 µM for VA, and 20 µM for DPZ. The solution of $A\beta_{1-42}$ (10 µM) with 50 µM PBS pH 7.4 was used. The $A\beta_{1-42}$ 10 µL was incubated with or without test compounds at 37°C for 48 h. After incubation period, 20 µM of 178 µL thioflavin T was added to previously incubated 96-well plate. The fluorescence intensities were measured at 450 nm (excitation) and 485 nm (emission) on microplate reader (SpectraMax M5, US). The Aβ aggregation assay samples were further used for confocal microscopic imaging (Carl Zeiss Microscopy GMBH, Germany) studies. After, 15 days of incubation period, all samples were mounted on glass slides using 1,4-diazabicyclo [2.2.2] octane (DABCO) as a fixing agent. Further, images were captured at 20X using fluorescence filter cube at 494 nm and 518 nm.

4.1.14. *In vitro* neuroprotection assay

The neuroprotective property of VAS was evaluated against $A\beta_{1-42}$ induced neurotoxicity on neuroblastoma cell line (SH-SY5Y) [168]. The cultured SH-SY5Y cells (density 1×10^5 cells/wells) were transferred into 96 well plates. Then, the cells were incubated (24 h at 37°C) in a humidified atmosphere under 5 % CO_2 condition. Further, cells were treated with 10 µM of $A\beta_{1-42}$ for the next 24 h. The test compound VAS (10, 20, 30 µM) cytotoxicity was evaluated against a VA (30 µM), DPZ (20 µM) was added, and cells were incubated for another 72 h. After that, 20 µL of MTT reagent was added into wells and incubated for an additional 2 h. As it results, purple-coloured formazan crystals were solubilized into 100 µL of DMSO to evaluate absorbance at 570 nm, and % cell viability was calculated.

4.1.15. Experimental animals and study design

The male Wistar rats (220 ± 15 g weight) were obtained from the Institute of Medical Science, Banaras Hindu University, Varanasi. The animals were housed in the environmentally controlled conditions of a 12 h. day/night cycle, temperature (25 ± 2°C), and humidity (55 ± 10 RH) at Animal House, Department of Pharmaceutical Engineering and Technology, Indian Institute of Technology (BHU), Varanasi. Animals were allowed to acclimatize for 7 days. All the experimental protocols were approved (approval no. Dean/2019/IAEC/1643) by the Institutional Animal Ethical Committee, Banaras Hindu University, Varanasi. The animal experiments are further divided into three different sets of experiments. The first set of experiments was designed to assess of acute oral toxicity of isolated compounds. The second set of experiments involved the evaluation of memory enhancement by isolated compounds against scopolamine-induced memory deficits. The third set of experiments was carried out to assess neuroprotection, cognitive, and memory enhancement activity of isolated compounds against Aβ induced AD.

4.1.16. Acute oral toxicity

Acute toxicity was evaluated by following OECD 423 guidelines [180]. The acute toxicity studies were performed on female rats (n = 6) by administering the VAS and VA (300 mg/kg) orally. After 14 days of test compound administration, animals were killed, and organs were isolated (brain, liver, kidney, and heart). The transverse sections (10 μm) were cut using a cryostat (SLEE MEV, Germany) and mounted on glass slides, and stained with hematoxylin and eosin. The slides were observed under a microscope (Magnus MLX plus, India) at 10X resolution.

4.1.17. Scopolamine induced amnesia

The Y-maze test was conducted to assess working memory in rats. The animals were divided into seven groups and each group consists of six rats (n = 6) i.e., group 1 normal control, group 2 disease control, group 3 VAS (5 mg/kg p.o.), group 4 VAS (10 mg/kg p.o.), group 5 VAS (20 mg/kg p.o.), group 6 VA (20 mg/kg p.o.), group 7 DPZ (5 mg/kg p.o.). Groups 1 and 2 received 0.5 % carboxy methyl cellulose (vehicle alone) for 7 days. Groups 3, 4, and 5, were treated with VAS, and group 6 was treated with VA for up to 7 days. Group 7 received DPZ orally for 7 days. On the 7^{th} day, after 30 min of final dose administration, scopolamine (0.5 mg/kg, i.p.) was injected into respective groups. Further, 30 min post administration of scopolamine-induced animals were tested on Y-maze apparatus for 5 min. The animals were placed at the center of the arm and allowed to explore for 5 min. When rat passes through all four paws into each arm was considered arm entry. The improvement in learning and memory is directly proportional to the increased spontaneous alterations (three consecutive arm entries). The percentage of spontaneous alternations was noted and calculated by using following formula percentage of spontaneous alternations: [number of alterations/ (total arm entries-2) ×100] [181].

4.1.18. Morris water maze test

The Morris water maze (MWM) test was performed to assess spatial learning and memory in rats [182]. The rats were randomly divided into five groups (n = 6): normal, Aβ control, VAS (20 mg/kg p.o.), VA (20 mg/kg p.o.), and DPZ (5 mg/kg p.o.). Animals were anesthetized using i.p. injection with a mixture of ketamine and xylene (dose of 90 and 9 mg/kg). Then, rats were placed into stereotaxic apparatus, ear bars were fixed and the scalp was incised and retracted. The head position was adjusted to locate the bregma and lambda region. The stereotaxic co-ordinates were set to bregma (-0.5 mm anteroposterior, +1.2 mm mediolateral, -3.2

dorsoventral and incision bar was set at -3.3 mm). Next, previously prepared $A\beta_{1-42}$ sterile saline injection (4 µM, 5µL) was infused into all groups except sham group through a Hamilton micro syringe at a flow rate of 2 µL/min. The syringe was kept for another 5 minutes to prevent efflux of infused solution. In sham group, saline was infused in the place of $A\beta_{1-42}$. All the animals were kept under special care after surgery was done.

After seven days of stereotaxic injection, test drugs VAS and VA treatment was given for next seven days. Further, the spatial memory in rats was investigated using MWM test. The MWM test apparatus (62 cm height, 32 cm depth, and 121 cm diameter) was equally divided into four quadrants filled with water (25 ± 2°C) and titanium dioxide was used to make water opaque. MWM test was divided into two trials, the first trial is a training trial, where animals find a hidden platform in one of the quadrants (5 days, 4 trials per day, intra-trail interval of about 10 min), and on the 6th day, a probe trial, where the platform was removed and animals are allowed to find the location of the platform as a spatial memory recognition (Figure 4.2). The duration for both trials was conducted for 2 min.

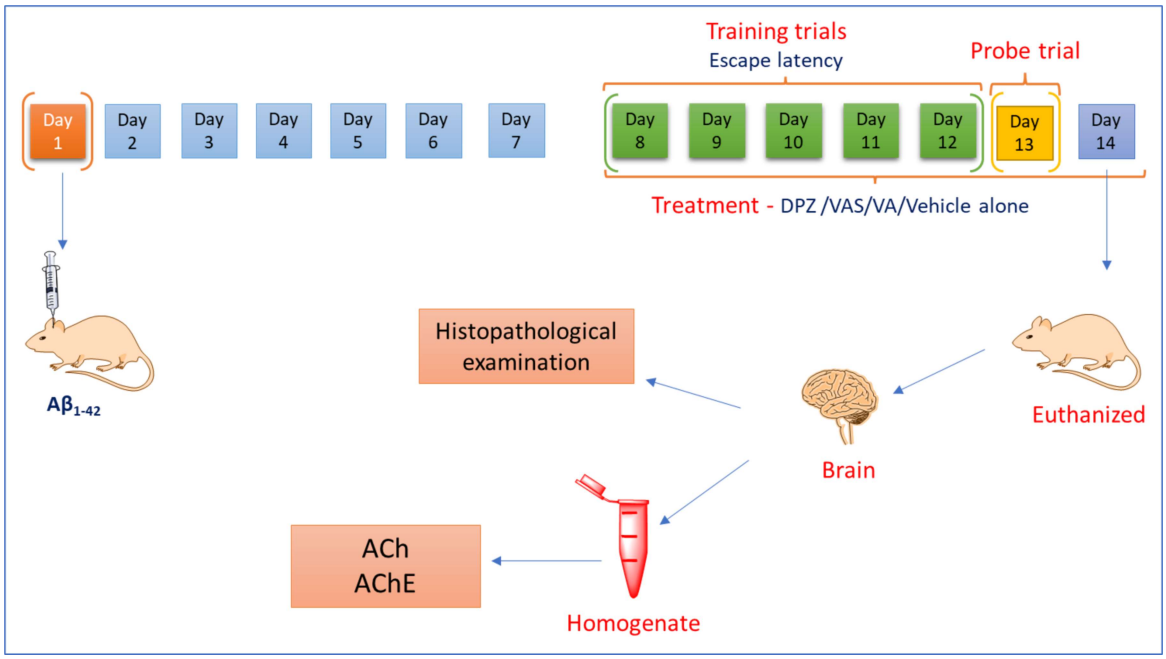

Figure 4.2. The schematic representation of Aβ induced Alzheimer's model study design

4.1.19. AChE, ACh estimation, and Histopathological studies

All groups of animals were euthanized after completion of behavioral studies, and whole brain was isolated from each animal. The brain samples were homogenized with 10 mM phosphate buffer solution (pH 7.4) and centrifuged (4°C) at 4350 g for 15 min. The obtained supernatants were separated and used for AChE estimation as per Ellman method [183]. Further, Acetylcholine (ACh) levels were measured using a rat acetylcholine estimation ELISA kit (Krishgen Biosystems, India). Estimation of AChE, 100 µL of supernatant was incubated with 15 mM of 100 µL ATCI (prepared in PBS buffer 7.4) for 5 min. Followed by addition of 100 µL of 1.5 mM DTNB and absorbance was measured at 415 nm. The rate of hydrolysis was calculated as µM of substrate hydrolyzed/min/mg of protein.

The whole brain of all animals was isolated for evaluating neuronal cell density in the hippocampus. The brains were washed with saline and fixed in 4 % paraformaldehyde solution at 4°C overnight. Then, kept in 15 % of sucrose solution (in PBS) and 30% sucrose (in PBS). Next, embedding was done in an optimum cutting temperature (OCT) solution 10 µm thick transverse sections were cut by a cryostat (SLEE MEV) and mounted on poly-L-lysine coated slides. These sections were hydrated in 95 % ethyl alcohol solution at room temperature for 5 h, rinsed in 75 % of ethyl alcohol for 5 min, and then distilled water for another 5 min. After, incubated in 1 % cresyl violet acetate (warmed at 50 - 60° C) for 20 min, rinsed in water for 5 min, and dehydrated at 75 % alcohol for a few seconds, 95 % ethyl alcohol for 2 min, and then absolute alcohol for 2 min. Finally, they were cleared in xylene for 2-3 min and mounted with DPX and slides were observed under a microscope (Magnus MLX plus, India) at 4X and 10X magnification. The cell density and cell count of hippocampus regions (DG, CA3, and CA1) were calculated using ImageJ software (NIH, USA) [184].

4.1.20. Statistical analysis

The statistical data were expressed in mean ± standard deviation (S.D). Graph pad prism 5 software was used to analyze the experimental data. All the results were analyzed by one-way ANOVA followed by Tukey's post hoc test, except escape latency in MWM, which was analyzed by two-way ANOVA followed by Bonferroni's post hoc test. A P-value of less than 0.05 was considered statistically significant.

4.2. Results

4.2.1. Chemical and structural properties of isolated compounds

The AVME (green, semi-solid) yield was found to be 12.35 % w/w from dry leaves of AV. The DCM fraction of AVME extraction produced high yield, i.e., 13.54 % w/w than, hexane (10.17 % w/w), butanol (9.33 % w/w), toluene (6.72 % w/w), and ethyl acetate (4.56 % w/w). In DCM fraction, two phytoconstituents were isolated using column chromatography and were identified as VAS (yield, 0.451 % w/w) and VA (yield, 4.37 % w/w). The compound VAS was eluted from fraction numbers 62-75 at mobile phase polarity of DCM: methanol (99:1). While VA was eluted from fractions 102-134 at polarity of DCM: methanol (96:4).

VAS (Figure 4.3) is characterized by a solid, pale yellow colour, characteristic odour, and a melting point of 199 $^{\circ}$C. ^{1}H NMR: (500 MHz, $CDCl_3$) δ 8.31 (dd, J = 6.8, 5.8 Hz, 1H), 7.90 – 7.62 (m, 2H), 7.53 – 7.46 (m, 1H), 5.35 – 5.20 (m, 1H), 4.48 – 4.26 (m, 1H), 4.06 – 4.01 (m, 1H), 2.76 – 2.62 (m, 1H), 2.40 – 2.28 (m, 1H), 1.98 (s, 1H). ^{13}C NMR: (125 MHz, $CDCl_3$) δ 160.6, 148.4, 142.9, 134.4, 126.9, 126.6, 126.5, 71.7, 55.8, 43.4, 29.3. The HRMS of $[M+H]^+$ was calculated as 203.0821 and found to be 203.0797, for $C_{11}H_{11}N_2O_2$. HPLC purity of VAS was estimated as 98%.

VA (Figure 4.3) was identified as dull brown colour, solid, and characteristic odour, and a melting point of 209 °C. ^{1}H NMR: (500 MHz, $CDCl_3$) δ 7.21 – 7.09 (m, 2H), 7.05 – 6.97 (m, 1H), 6.89 (d, *J* = 7.5 Hz, 1H), 4.96 (s, 1H), 4.83 – 4.80 (m, 1H), 4.68 – 4.55 (m, 2H), 3.48 – 3.42 (m, 1H), 3.30 – 3.25 (m, 1H), 2.45 – 2.36 (m, 1H), 2.16 – 2.08 (m, 1H). ^{13}C NMR: (125 MHz, $CDCl_3$) δ 163.8, 141.3, 128.5, 125.9, 124.5, 123.2, 118.7, 70.2, 48.6, 47.1, 28.7. The HRMS of $[M+H]^+$ was calculated as 189.1028 and found to be 189.1000, for $C_{11}H_{13}N_2O$. HPLC purity of VA was estimated as 99 %.

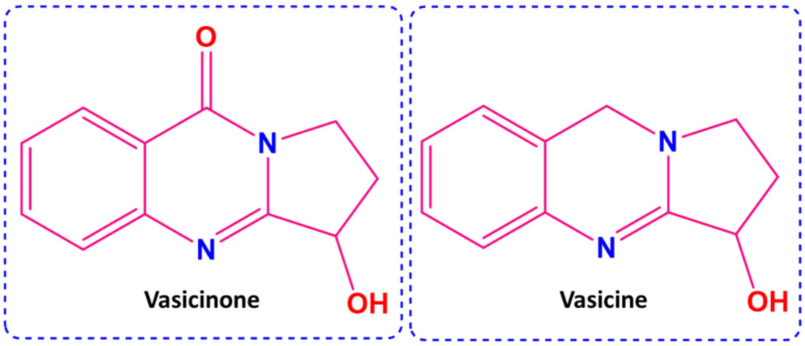

Figure 4.3. The structures of pyrroloquinazoline alkaloids isolated from *Adhatoda vasica* Nees.

4.2.2. Drug-likeness, ADME, and toxicity parameters

ADME prediction of screened compounds revealed that VAS and VA are obeying Lipinski's rule of five. Further, we found that VAS and VA displayed better human intestinal absorption (HIA) and exhibits low skin permeability. The results showed, no predicted toxicity in mice and rats. The cardiotoxicity (hERG) prediction indicates that low risk against hERG channel. The obtained results were listed in supplementary information (Table 4.1).

Table 4.1. Drug-likeness and ADMET properties of VAS and VA

Parameters	VAS	VA
Mol. Wt.	202.21	188.23
Log p	1.01	1.17
TPSA[a]	55.12	35.83
HBA[b]	3	2
HBD[c]	1	1

RBS[d]	0	0
HIA[e] (%)	94.8589	95.471
Coco2[f] (nm/s)	20.697	29.3183
MDCK[g] (nm/s)	3.5007	278.649
SP[h] (log $k_{p,}$ cm/h)	-4.211	-3.868
PPB[i] (%)	70.0346	80.3315
P-gp inhibition	Non	Non
CYP3A4 inhibition	Non	Non
CYP 2C9 inhibition	Non	Non
CYP 2C19 inhibition	Non	Non
CYP 2D6 inhibition	Non	weakly
Ames's test	Mutagen	Mutagen
Carcinogenicity (rats)	Negative	Negative
Carcinogenicity (mouse)	Negative	Negative
HERG inhibition	Low risk	Low risk

[a] topological polar surface area; [b] H bond acceptor; [c] H donor; [d] rotatable bonds, [e] human intestinal absorption, [f] *in-vitro* Coco2 cell permeability, [g] Madin-Darby canine kidney permeability, [h] *in-vitro* skin permeability, [i] *in-vitro* plasma protein binding.

4.2.3. Molecular docking studies on AChE

The binding interaction of VAS and VA at active site of AChE was depicted in Figure 4.4. The docking parameters were validated by superimposed position with its crystalized conformer donepezil at the active site of AChE. The compound VAS and VA formed interactions with AChE active site and showed low binding energies (Table 4.2). It was observed that VAS and VA interacted with several key amino acid residues present in the active site of AChE by forming multiple chemical bonds like hydrogen bonds, π-π stacked, and π-alkyl. These interactions were similar to reference compound DPZ (Figure 4.4).

Table 4.2. Displaying interactions of ligands with AChE, BuChE, and binding energies

S. No.	Compound	AChE		BuChE	
		Binding Energy (Kcal/mol)	**Amino acid Interaction**	**Binding Energy (Kcal/mol)**	**Amino acid Interaction**
1	VAS	-6.98	Phe295 (H-bond), Trp286 (π-π stacked), Tyr341 (π-π stacked), Tyr124 (π-π t-shaped), Trp286 (π-alkyl)	-6.26	Ser198 (H-bond), Ser198 (H-bond), His438 (H-bond), Trp231 (π-π, t-shaped), Phe329 (π-π, t-shaped), Gly116 (amide-π stacked), Gly117 (amide-π stacked)
2	VA	-6.62	Phe295 (H-Bond), Phe296 (H-Bond), Tyr124 (π-π), Tyr341 (π-π), Trp286 (π-alkyl)	-5.93	Trp430 (H-bond), Tyr440 (H-bond), Trp82 (π-π stacked, π-alkyl), Ala328 (alkyl), A: TRP430 (π-alkyl), Tyr440 (π-alkyl)
3	DPZ	-11.8	Trp86 (π-π stacked), Arg296 (H-bond), Trp286 (π-π stacked, π-Alkyl), Ser293(H-bond), Leu298 (alkyl), Tyr337 (π-alkyl), Phe338 (π-alkyl), Tyr341 (H-bond)	-	-
4	Tacrine	-	-	-6.75	Gln67 (H-bond), Ile69 (π-alkyl), Trp82 (H-bond, π-alkyl), Thr120 (π-σ)

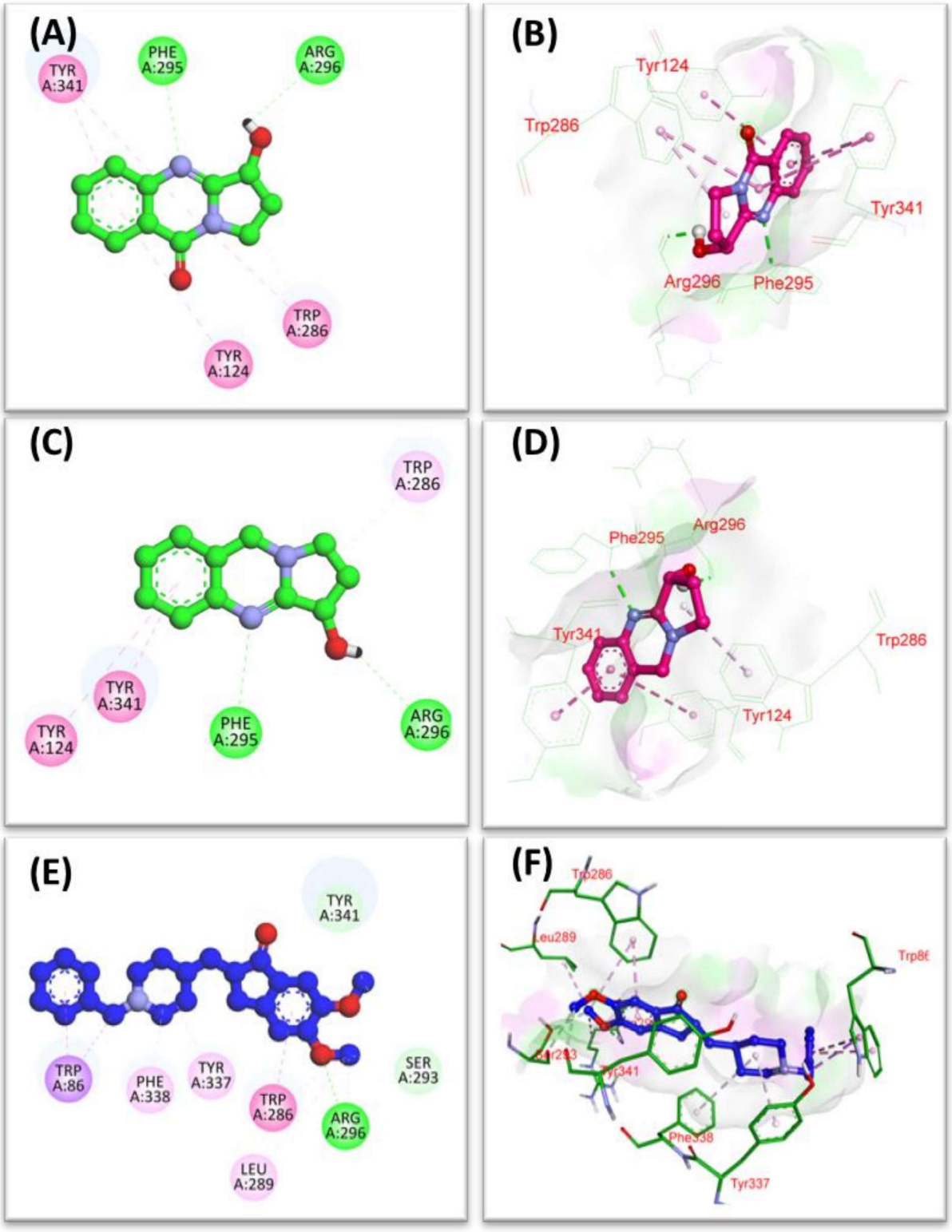

Figure 4.4. The binding interactions of VAS, VA, and DPZ at AChE active site. (A) and (B), depicts the interaction of VAS with AChE, (C) and (D) depicts the interaction of VA with AChE, and (E) and (F) depicts the interaction of DPZ with AChE.

4.2.4. Molecular docking studies on BuChE

The compound VAS and VA showed interactions with BuChE at active site and showed low binding energies (Table 4.2). These ligands showed similar interaction profiles with reference compound tacrine (Figure 4.5). We observed that VAS and VA interacted with many key amino acid residues present in the active site of BuChE by forming various chemical bonds like hydrogen bonds, π-σ, and π-alkyl (Figure 4.5).

4.2.5. Molecular dynamics studies of VAS on AChE

The protein-ligand interactions were analyzed using following parameters, such as hydrogen bond interactions, hydrophobic interactions, ionic interactions, and water bridges formed between ligand and protein (Figure 4.6). The hydrogen bond interactions formed between compound VAS and AChE amino acid residues are Trp286, Glu292, Ser293, Phe295, Arg296, and Phe338. The hydrogen bond can influence drug specificity, adsorption, and metabolism. The observed hydrophobic interactions are Tyr72, Leu76, Tyr124, Trp286, Leu289, Phe297, Tyr337, Val340, and Tyr341. There no notable ionic interaction was found between AChE and VAS. The observed water bridges are Tyr72, His287, Gln297, Glu292, Ser293, Arg296, Ser298, Phe338, and Tyr341. The ligand RMSF, protein RMSF, protein-ligand contacts, protein RMSD, ligand RMSD, and properties of ligand VAS results were strongly suggesting that ligand VAS is most stable at AChE site (Figure 4.6).

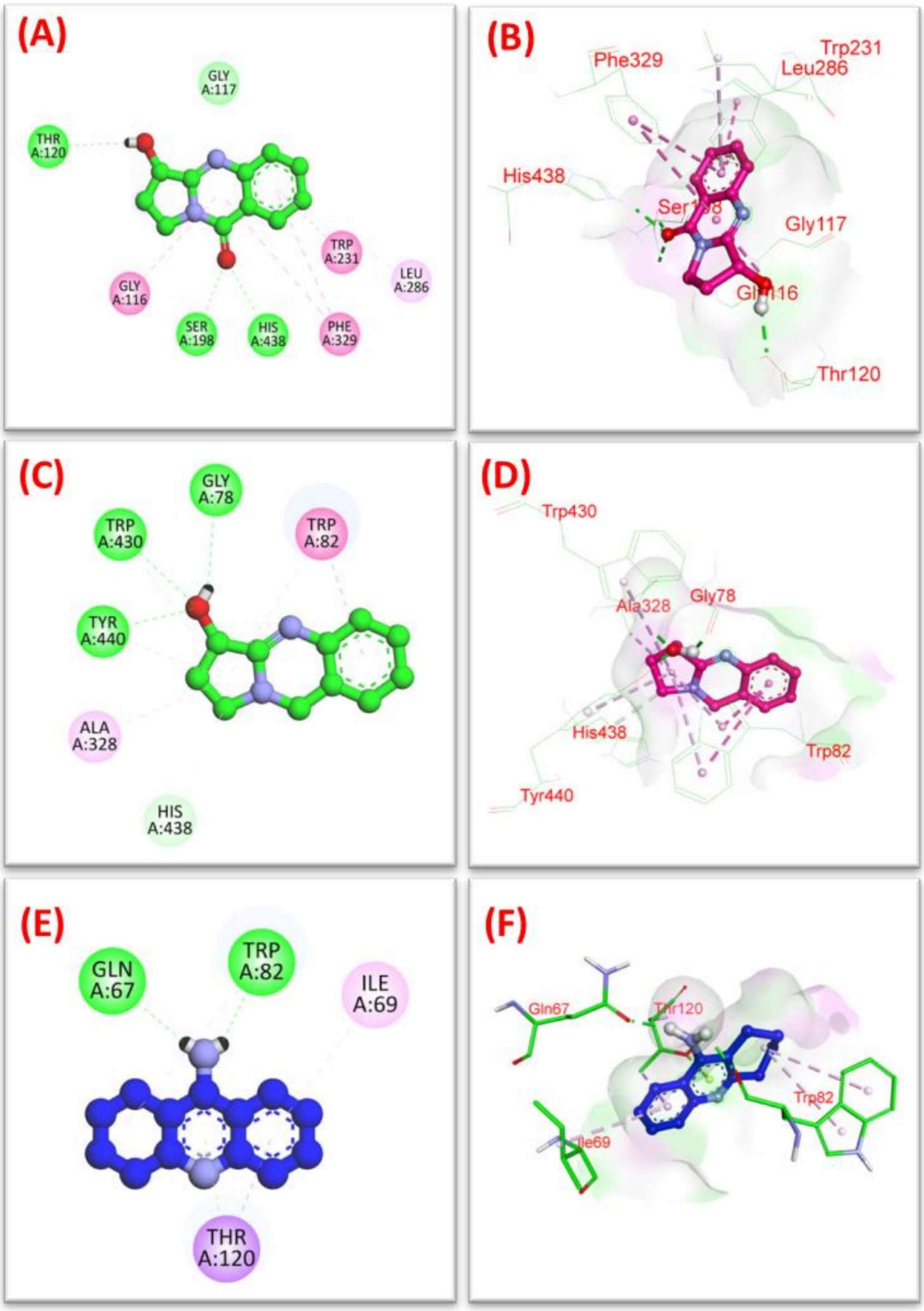

Figure 4.5. The binding interactions of VAS, VA, and DPZ at BuChE active site. (A) and (B), depicts the interaction of VAS with BuChE, (C), and (D) depicts the interaction of VA with BuChE, and, (E) and (F) depicts the interaction of tacrine with BuChE.

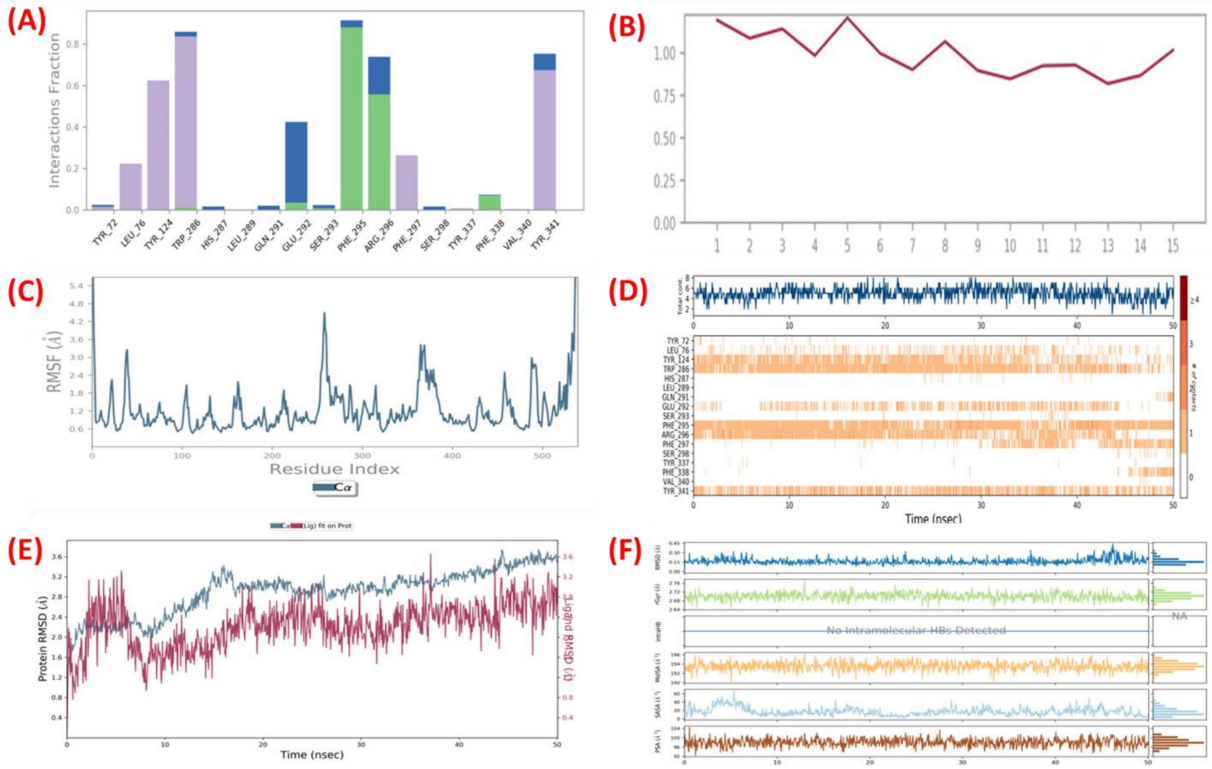

Figure 4.6. VAS modulates the AChE interactions on molecular dynamic simulations**,** (A) showing bar charts of ligand-protein interactions throughout the simulation (Green- H-bonding; Gray - hydrophobic; Blue - water bridges), (B) depicts the ligand VAS Root mean square fluctuation (RMSF) and stability at active site, (C) showing the RMSF plot of protein AChE during simulation, (D) depicts the AChE-VAS contacts during simulation, (E) depicts the protein root mean square deviation (RMSD) (left Y-axis) and ligand RMSD (right Y-axis) indicated the stability of ligand VAS with respect to protein AChE, and (F) showing Ligand VAS properties during simulation.

4.2.6. Molecular dynamics studies of VA on AChE

The compound VA showed stable hydrophobic interactions with AChE active site amino acids (Figure 4.7). They are Tyr72, Leu76, Tyr124, Trp286, His287, Leu289, Glu292, Phe297, Phe338, and Tyr341 which may play important roles in substrate binding. The ligand VA formed hydrogen bond interaction with Phe295 (100 % simulation time) and Arg296 (10 % simulation time). Water bridges formed between ligand and Phe338 residue. There is no ionic interactions were formed between protein and ligand VA. The ligand RMSF, protein RMSF,

protein-ligand contacts, protein RMSD, ligand RMSD, and properties of ligand VA results suggested that VA have stable interaction profile in the AChE active site (Figure 4.7).

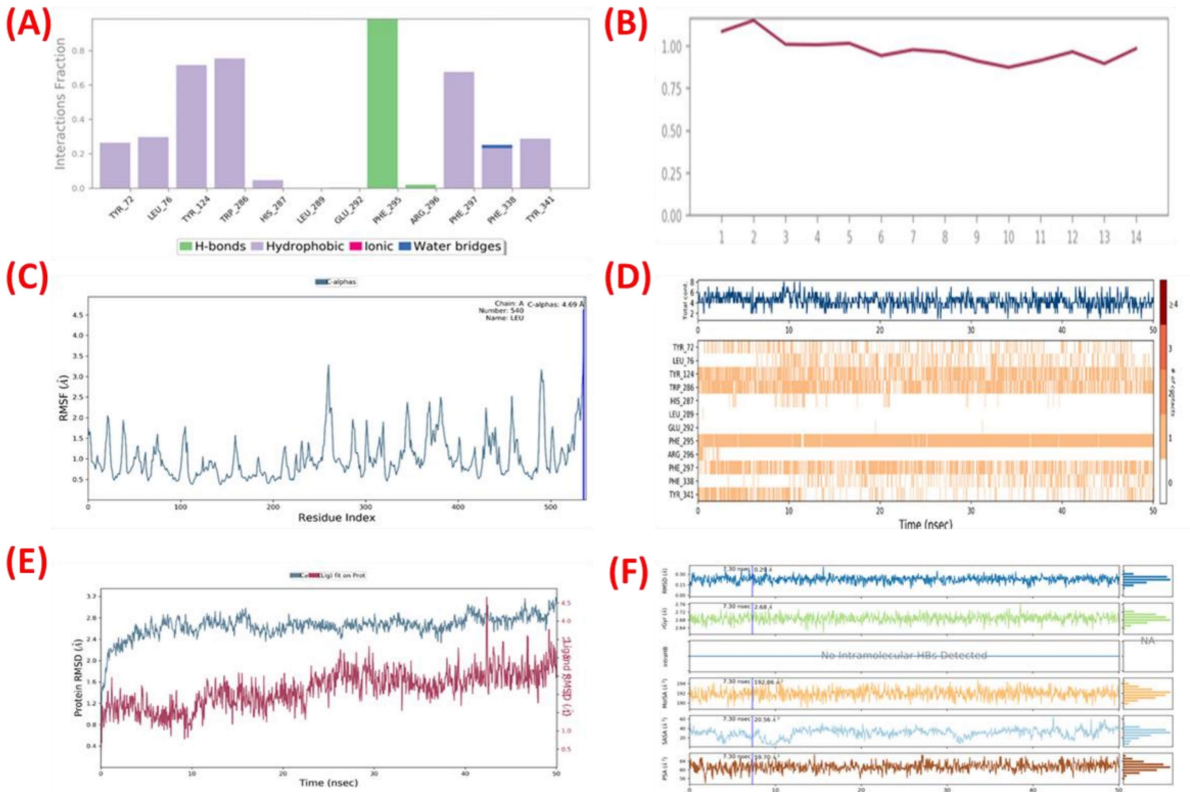

Figure 4.7. VA modulates the AChE interactions on molecular dynamic simulations**,** (A) showing bar charts of ligand-protein interactions throughout the simulation (Green- H-bonding; Gray- hydrophobic; Blue- water bridges), (B) depicts the ligand VA Root mean square fluctuation (RMSF) and stability at active site, (C) showing the RMSF plot of protein AChE during simulation, (D) depicts the AChE-VA contacts during simulation, (E) depicts the protein root mean square deviation (RMSD) (left Y-axis) and ligand RMSD (right Y-axis) indicated the stability of ligand VA with respect to protein AChE, and (F) Showing Ligand VA properties during simulation.

4.2.7. Cholinesterase inhibition activity

The IC_{50} values of AVME, fractions, VAS, and VA against AChE and BuChE, and antioxidant activities were depicted in Table 4.3 and Table 4.4. The DCM fraction (AChE IC_{50}: 18.37 ± 0.53 µg; BuChE IC_{50}: 30.22 ± 0.82 µg, DPPH IC_{50}: 65.71 ± 1.29 µg) has been identified as

highest cholinesterase inhibitory potency (Table 4.3). The IC_{50} values of isolated compound VAS (AChE IC_{50}: 3.26 ± 0.070 µM; BuChE IC_{50}: 5.62 ± 0.083 µM, DPPH IC_{50}: 30.44 ± 0.47 µM) and VA (AChE IC_{50}: 2.97 ± 0.061 µM; BuChE IC_{50}: 5.03 ± 0.073 µM, DPPH IC_{50}: 34.12 ± 0.43 µM) showed promising results on AChE and BuChE enzymes (Table 4.4). These results indicate that DCM fraction containing VAS and VA exhibited significant inhibition on AChE ($P < 0.05$) and BuChE ($P < 0.05$), and DPPH ($P < 0.005$) assays.

Table 4.3. Effect of AV extract and its fractions on AChE, BuChE, and DPPH inhibitory activity

S. No.	Extract/ Fraction	eeAChE IC_{50} (µg) [a]	eqBuChE IC_{50} (µg) [a]	DPPH IC_{50} (µg) [a]
1	Methanolic extract	48.35 ± 1.37	70.41 ± 1.63	100.27 ± 2.08
2	Hexane fraction	78.67 ± 1.49	91.91 ± 2.35	165.16 ± 2.64
3	Toluene fraction	54.14 ± 1.00	70.28 ± 2.06	144.31 ± 2.45
4	Ethyl acetate fraction	39.30 ± 0.86	52.29 ± 1.28	121.43 ± 2.18
5	DCM fraction	18.37 ± 0.53	30.22 ± 0.82	65.71 ± 1.29
6	Butanol fraction	36.46 ± 1.01	49.16 ± 1.34	101.58 ± 1.49

[a] Data expressed in three independent experiments (mean ± SD, n = 3)

Table 4.4. Effect of VAS and VA on AChE, BuChE, and DPPH inhibitory activity

S. No.	Compound	eeAChE IC_{50} (µM) [a]	eqBuChE IC_{50} (µM) [a]	DPPH IC_{50} (µM) [a]
1	VAS	3.26 ± 0.070	5.62 ± 0.083	30.44 ± 0.47
2	VA	2.97 ± 0.061	5.03 ± 0.073	34.12 ± 0.43
3	DPZ	0.048 ± 0.00056	0.13 ± 0.0032	nd
4	AA	nd	nd	26.16 ± 0.38

[a] Data expressed in three independent experiments (mean ± SD, n = 3). nd = not determined, DPZ = donepezil, AA = ascorbic acid.

4.2.8. PAMPA-BBB assay

The BBB permeation of tested compounds was predicted [185] by following indications $P_e > 4.0 \times 10^{-6}$ cm s^{-1} could cross BBB (CNS+), $P_e < 2.0 \times 10^{-6}$ cm s^{-1} not cross the BBB (CNS-), and compounds with 2.0×10^{-6} cm $s^{-1} < P_e > 4.0 \times 10^{-6}$ cm s^{-1} uncertain BBB permeation (CNS±). The permeability of VAS and VA was found to be $5.61 \pm 0.12 \times 10^{-6}$ cm s^{-1} and $5.21 \pm 0.11 \times 10^{-6}$ cm s^{-1} respectively. These results suggested that compounds (VAS and VA) can cross BBB.

4.2.9. Aβ aggregation studies

The inhibitory effects of VAS and VA on Aβ aggregation were depicted in Figure 4.8. Compounds VAS and VA, exhibited moderate anti-aggregatory properties at a concentration of 10 μM and 20 μM in Aβ aggregation assay (Figure 4.8). At, 30 μM concentration, compounds showed promising results and there is no significant difference with positive control DPZ (20 μM) ($P < 0.0001$). Aβ (control) samples showed large-size aggregates and treated samples showed small-size aggregates confirmed by confocal imaging studies. The confocal images were taken at VAS/VA of 30 μM concentrations, which has shown significant Aβ inhibition.

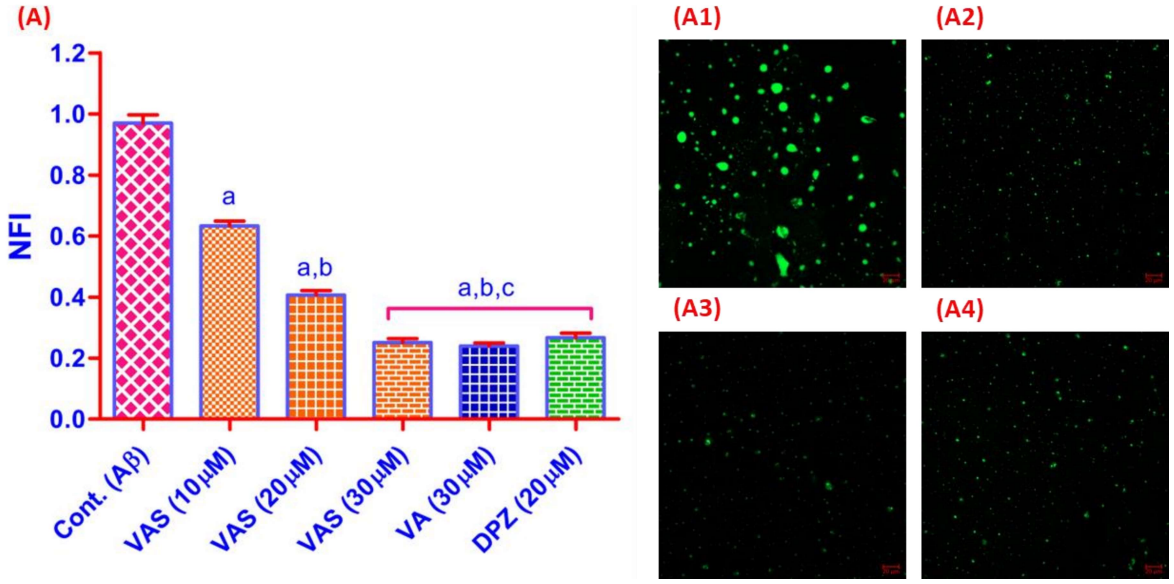

Figure 4.8. Effect of VAS and VA on Aβ aggregation. (A) showing inhibitory effect of isolated compounds on Aβ aggregation, (A1) showing effect of Aβ aggregates without isolated compounds, (A2) showing effect of VAS (30 μM) on Aβ aggregates, (A3) showing effect of VA (30 μM) on Aβ aggregates, and (A4) showing effect of DPZ (20 μM) on Aβ aggregates. $^{a}P<0.05$ compared to control, $^{b}P<0.05$ compared VAS (10 μM), $^{c}P<0.05$ compared VAS (20 μM). (Mean ± SD, n=3. One-way ANOVA followed by Tukey's post hoc test). NFI: nominal fluorescence intensity.

4.2.10. Propidium iodide displacement assay

The test compounds VAS and VA affinity towards the peripheral anionic site (PAS) of AChE results were presented in Figure 4.9. The propidium iodide fluorescence was decreased in the presence of VAS/VA, which suggested that compounds can be interrupted by propidium displacement from the PAS site. The obtained results of VAS and VA were significant ($P < 0.0001$) to reference drug DPZ.

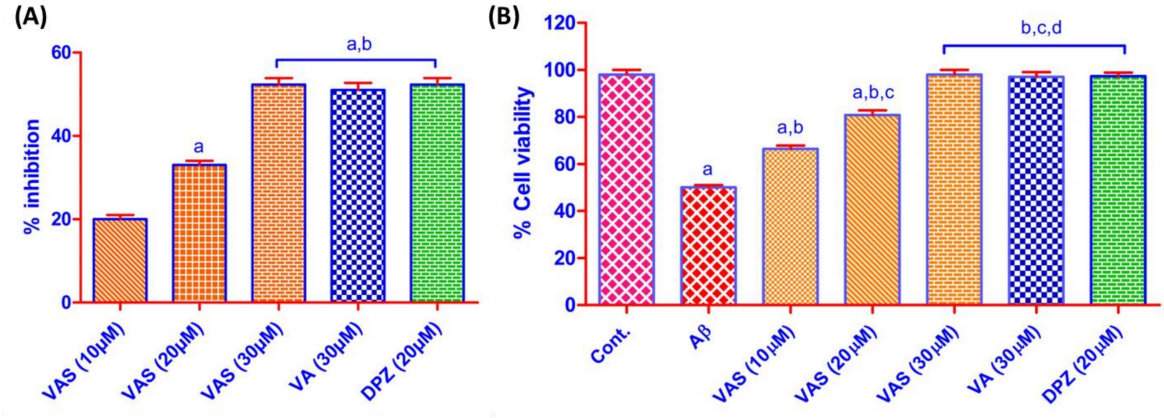

Figure 4.9. Effect of VAS and VA on propidium iodide displacement assay and neuroprotection activity. (A) depicts the effect of VAS and VA on propidium iodide displacement. $^{a}P < 0.05$ compared to VAS (10 µM), $^{b}P < 0.05$ compared to VAS (20 µM). (B) depicts the effect of VAS and VA on SH-SY5Y cells. $^{a}P < 0.05$ compared to control, $^{b}P < 0.05$ compared to Aβ, $^{c}P < 0.05$ compared to Aβ+VAS (10 µM), $^{d}P < 0.05$ compared to Aβ+VAS (20 µM). One-way ANOVA followed by Tukey's post hoc test (n=3).

4.2.11. Neuroprotection studies

The neuroprotective nature of VAS and VA against SH-SY5Y cells were depicted in Figure 4.9. Cell viability was increased in a dose-dependent manner by treatment with VAS and VA (Figure 4.9). The findings demonstrated that there is no significant difference between test compounds VAS (30 µM) and VA (30 µM) as compared to DPZ (20 µM) in cytotoxicity profile ($P < 0.0001$).

4.2.12. Acute oral toxicity

The acute oral toxicity studies of VAS and VA were illustrated in Figure 4.10. There were no notable toxicity symptoms observed i.e., behavioral changes, mortality, body weight, and changes in food and water consumption. Histological studies on different organs suggested that there was no significant histological damage in brain, liver, heart, and kidney at a dose of 300 mg/kg. The organ section images are shown as 10X using bright field microscope Figure 4.10.

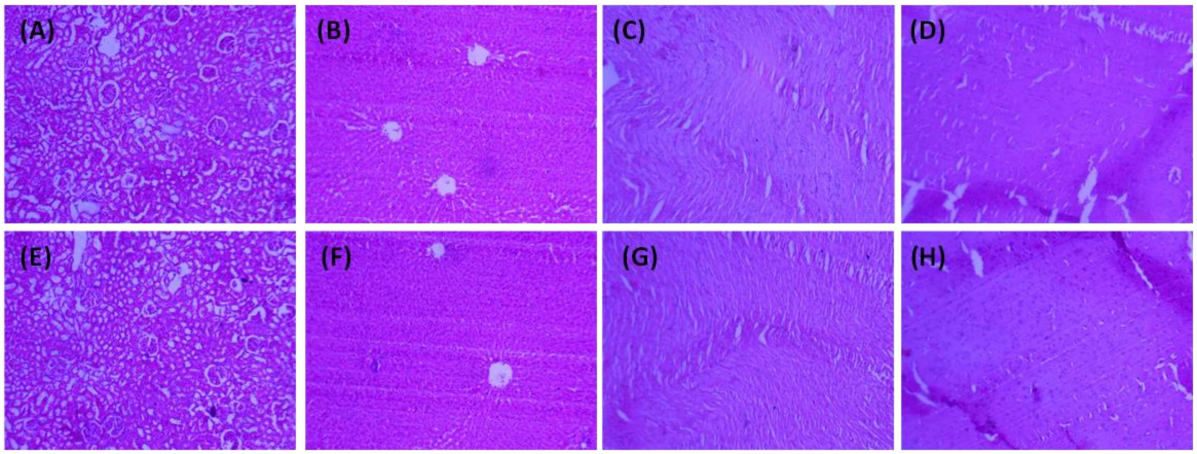

Figure 4.10. Effect of VAS and VA treatment on organ toxicity. A, B, C, and D indicates the effect of VAS treatment on histological abnormalities in kidney, liver, heart, and brain, respectively. E, F, G, and H indicates the effect of VA treatment on histological abnormalities in kidney, liver, heart, and brain, respectively.

4.2.13. Scopolamine induced amnesia

The changes in scopolamine-induced cognition and memory function with the treatment of VAS and VA are depicted in Figure 4.11. One-way ANOVA revealed significant differences among the groups [168]. The percentage of spontaneous alternations and ACh levels were decreased ($P < 0.0001$) while AChE activity was increased ($P < 0.0001$) in the scopolamine-treated rats than control rats ($P < 0.0001$). VAS and VA treatment significantly increased the spontaneous alternations (%) ($P < 0.0001$) and ACh levels ($P < 0.0001$); and decreased AChE activities ($P < 0.0001$) than scopolamine-treated groups. Further, there were no significant differences in spontaneous alterations (%) ($P < 0.0001$), AChE ($P < 0.0001$) activity, and ACh levels ($P < 0.0001$) between VAS, VA, and DPZ-treated groups. These findings indicate that VAS and VA significantly improved memory function in scopolamine-treated rats.

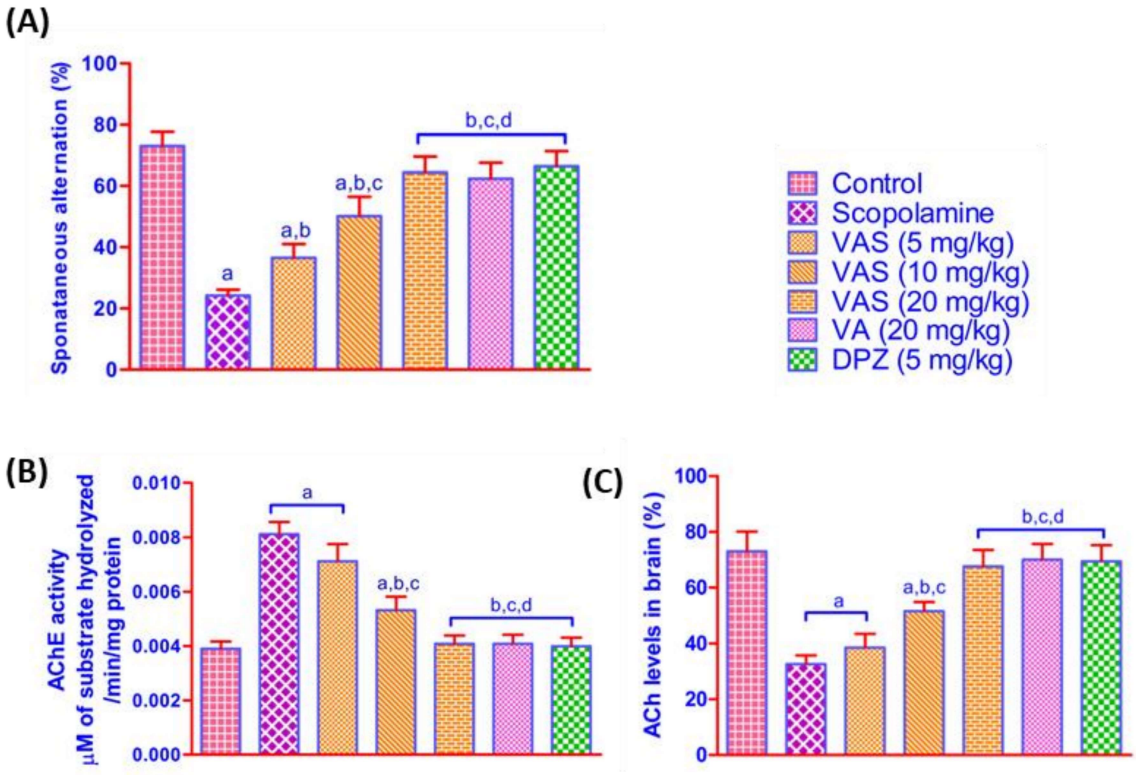

Figure 4.11. Effect of VAS on scopolamine-induced cognition and memory impairment. (A) showing effect of VAS on spontaneous alternations (%), (B) showing effect of VAS on AChE activity in the brain, and (C) showing effect of VAS on ACh levels in the brain. $^{a}P<0.05$ vs. control; $^{b}P<0.05$ vs. scopolamine; $^{c}P<0.05$ vs. VAS (5 mg/kg); $^{d}P<0.05$ vs. VAS (10 mg/kg). One-way ANOVA followed by Tukey's post hoc test, n=6.

4.2.14. Aβ induced Alzheimer's

The changes in Aβ induced memory deficits, AChE activity, and ACh levels after treatment with VAS and VA are depicted in Figure 4.12. Aβ treated rats significantly increased the escape latency ($P < 0.0001$) and AChE activity ($P < 0.0001$), and decreased time spent in the platform zone ($P < 0.0001$), number of entries into the platform zone ($P < 0.0001$), and ACh levels than control group ($P < 0.0001$). VAS and VA-treated groups significantly decreased the escape latency and AChE activity ($P < 0.0001$), and increased time spent in the platform zone ($P < 0.0001$), number of entries into the platform zone ($P < 0.0001$), and ACh levels in Aβ group (P

< 0.0001). The dose of VAS at 20 mg/kg (p.o.) showed significant effect when compared to VA (20 mg/kg, p.o.) and DPZ (5 mg/kg, p.o.) groups.

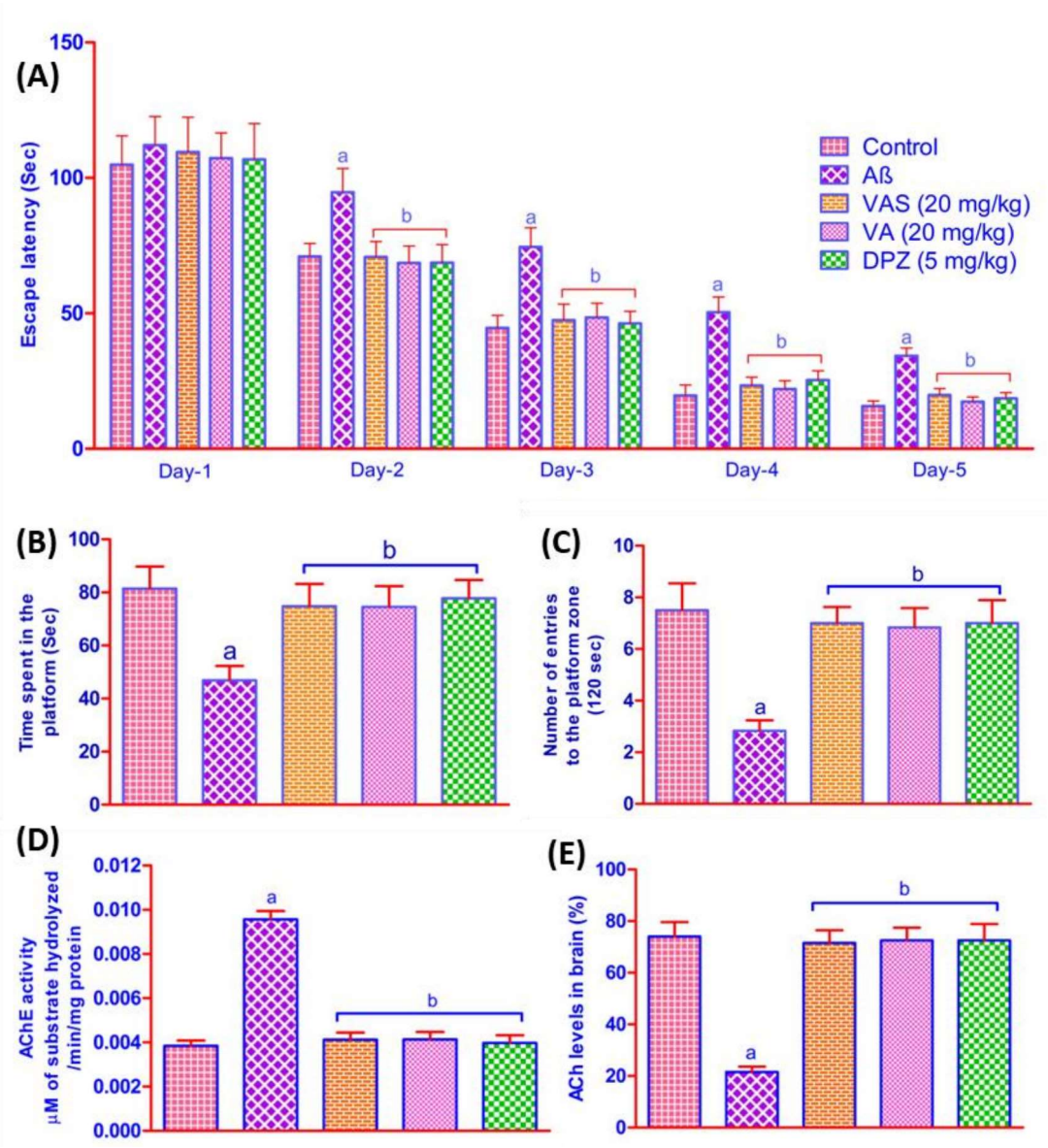

Figure 4.12. Effect of VAS and VA on Aβ induced memory deficits. (A) effect of VAS on escape latency during the training trials, (B) showing animals time spent on the platform during probe trial, (C) depicts the number of entries to the platform zone, (D) showing the effect of VAS on AChE in the brain, and Fig. 11E showing the effect of VAS on ACh in the brain. $^{a}P<0.001$ compared to normal control, $^{b}P<0.05$ compared to Aβ control. One-way ANOVA followed by Tukey's post hoc test (n=6).

4.2.15. Histological studies

The changes in the neuronal cell density by treatment with VAS and VA against Aβ induced memory deficits in rats were illustrated in Figure 4.13. Aβ group showed lower number of neuronal cells and neuronal cell density (%) in DG, CA1, and CA3 regions of hippocampus than control groups ($P < 0.0001$). VAS/VA/DPZ treated groups increased the number of neuronal cells and neuronal cell density (%) in DG, CA1, and CA3 regions of hippocampus than Aβ group ($P < 0.0001$) (Figure 4.14). However, these parameters did not show any significant differences between VAS/VA/DPZ groups. These findings indicate that treatment with VAS and VA significantly increased ($P < 0.0001$) the neuronal density in Aβ group rats.

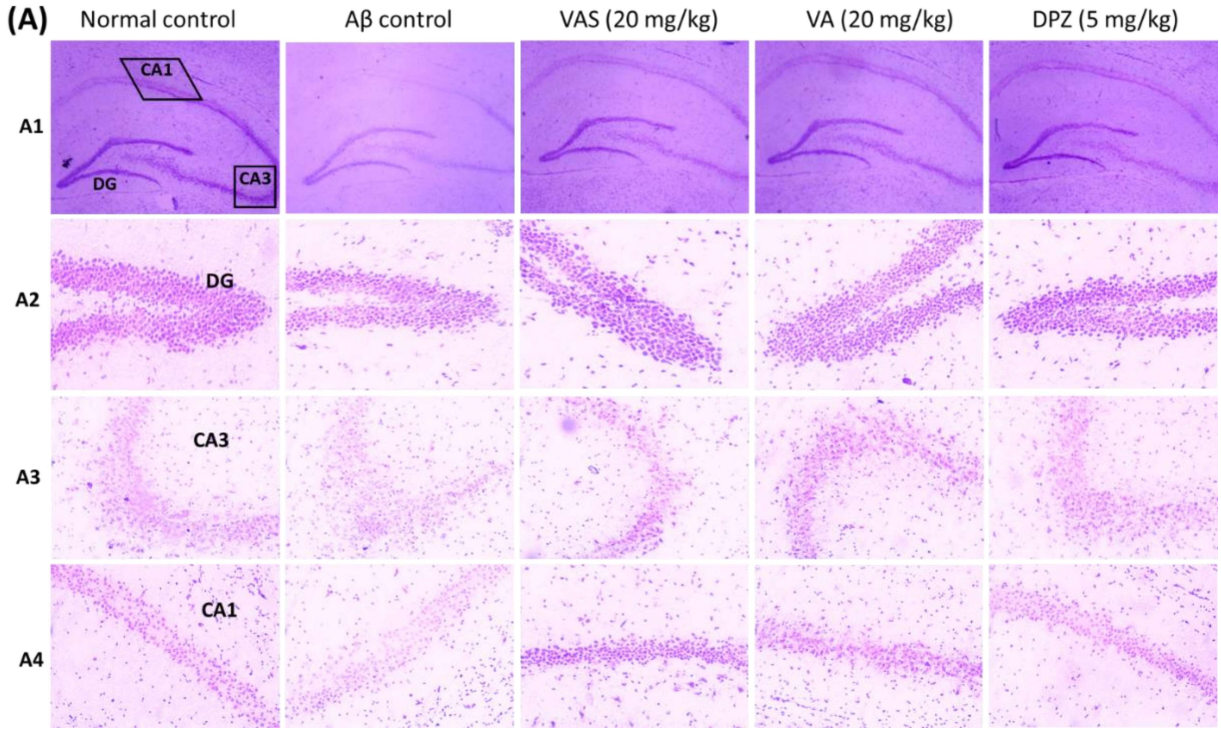

Figure 4.13. (A1) Indicates the neuronal density at hippocampus regions. (A2), (A3), and (A4) indicates neuronal cell density at dentate gyrus (DG), cornu ammonis 3 (CA3), and cornu ammonis 1 (CA1) respectively. The organ sections were reported in 4X and 10X resolution using bright field microscope (Nissl staining).

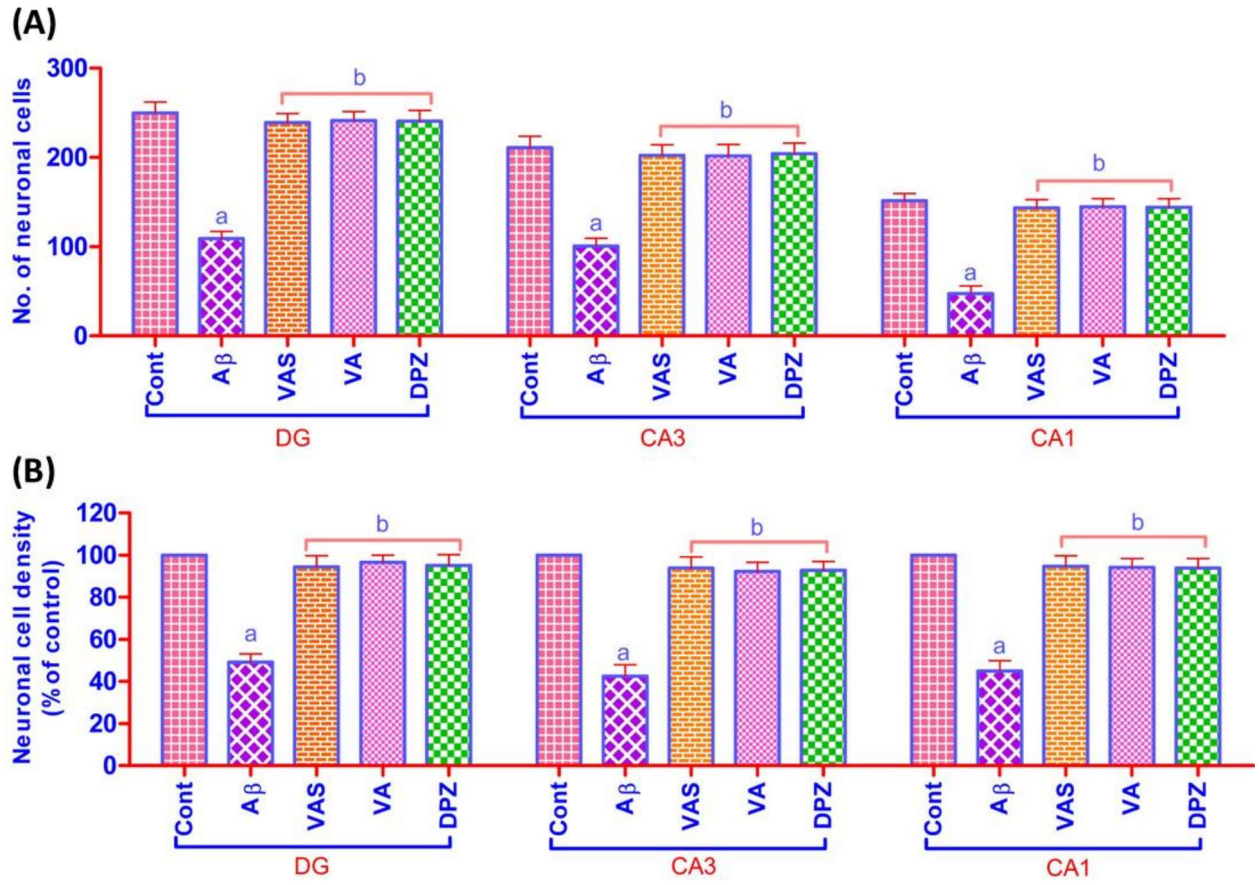

Figure 4.14. (A) The number of neuronal cells and (B) Neuronal cell density (% of control). [a]P<0.05 vs. normal control, [b]P<0.05 vs. Aβ control. One-way ANOVA followed by Tukey's post hoc test (n=6).

4.3. Conclusion

The present study identified two potent leads vasicinone (VAS) and vasicine (VA) from DCM fraction of AVME for the management of AD, compounds were screened through *in-silico, in-vitro,* and *in-vivo* studies. *In-silico* studies showed effective and stable binding interactions at AChE and BuChE active sites. These compounds VAS and VA effectively inhibited the AChE, BuChE, and Aβ aggregation in *in-vitro* studies. Further, Binding ability at AChE active site was confirmed by propidium iodide assay. The compounds were also exhibited antioxidant potency in *in-vitro* DPPH assay. Furthermore, compound neuroprotection potency was estimated in Aβ induced SH-SY5Y cell line. Moreover, *in-vivo* studies revealed that VAS and

VA enhanced working and spatial learning memory by enhancing the ACh levels and preventing hippocampal neuronal loss. The promising data from the *in silico*, *in vitro,* and *in vivo* experiments led us to report that both VAS and VA are potent natural drugs for the development of disease-modifying agents in AD. The work provided new evidence on VAS which acts multi-target manner in the treatment of AD.